

**Surveillance of Agricultural Drought Worldwide from Space using the
FAO-Agriculture Stress Index System (ASIS)**

Oscar Rojas,

**Climate and Environment Division, Food and Agriculture Organization of United
Nations, Rome, Italy**

Paul Racionzer, Yayun Li

**Trade and Markets Division, Food and Agriculture Organization of United Nations,
Rome, Italy**

Shukri, Ahmed ,

**Resilience Management Programme Team, Food and Agriculture Organization of
United Nations, Rome, Italy**

Herman Eerens, Roel Van Hoolst,

**Centre for Remote Sensing and Earth Observation, Flemish Institute for
Technological Research, Mol, Belgium**

Antoine Royer, Felix Rembold

Joint Research Centre of European Commission, Ispra, Italy

Lieven Bydekerke,

**Strategy and International Relations, European Organisation for the Exploitation of
Meteorological Satellites, Darmstadt, Germany**

Anton Vrieling,

Department of Natural Resources, University of Twente, The Netherlands

Abstract

FAO-Global Information and Early Warning System (GIEWS) and the Climate and Environment Division (CED) have developed an “*Agricultural Stress Index System*” (ASIS) for detecting agricultural areas with a high likelihood of water stress (drought) on a global scale using remote sensing data with the technical assistance and advice from the Flemish Institute for Technological Research (VITO-TAP) and the Monitoring Agricultural Resources (MARS) unit of the Joint Research Centre (JRC) of European Commission (EC). Data from NOAA-AVHRR and METOP-AVHRR (normalized difference vegetation index and brightness temperature) are used to calculate the per-pixel VHI on a global scale, averaged over the growing season. A phenological model, based on NDVI, is developed and employed to define the start and end of the growing season. Next, the averaged VHI (temporal integration) over the growing season is aggregated over each administrative unit so the drought intensity can be assessed on spatial basis. The resulting data flow will provide timely and direct information on drought stress in all agricultural areas of the world. ASIS would help to identify regions experiencing unfavourable crop growing conditions and food supply shortfalls and to determine food insecure areas and/or populations. ASIS assesses the severity (intensity, duration and spatial extent) of the agricultural drought and indicates the final results at administrative level giving the possibility to compare it with the agricultural statistics of the country. Currently the ASIS database contains 30+ years of agricultural hot spots data and information, starting from 1984.

1. Introduction

Drought is the world's most destructive natural hazard and has had devastating impacts on food security and food production. In 2011, the horn of Africa has faced the worst drought in 60 years (Wooldridge, 2011). An estimated 12.4 million people suffered from a massive food shortage. In 2012, the United States, world's largest maize and soybean producer, experienced its worst drought in over 50 years (Starita *et al*, 2012). The effects of the US drought combined with a wide spread drought in large areas of the Black Sea region (Russia, Ukraine and Kazakhstan), impacted prices and food security in many parts of the world. Episodes of drought increased in frequency and intensity over the past two decades as a result of climate change, and this trend is expected to continue (IPCC, 2012). To mitigate the impact of agricultural drought, it is of high importance to dispose of timely and reliable information of the condition of food crops in all regions and countries in the world. The Global Information and Early Warning System (GIEWS) and Climate and Environmental Division (CBC) of FAO had developed an "Agricultural Stress Index System" (ASIS) for detecting agricultural areas with a high likelihood of water stress (drought) on a global scale using remote sensing data. GIEWS monitors food supply and demand conditions for all countries in the world on a continuous basis and provides timely warnings of imminent food shortages, droughts, and hunger at individual country or sub-regional level. As part of its activities, the System collects and archives information from many different sources. It makes use of geographical information system (GIS) and remote sensing technologies to identify regions experiencing unfavourable crop growing conditions and food supply shortfalls and to determine food insecure areas and/or populations. ASIS was implemented on behalf of FAO by the Flemish Institute for Technological Research (VITO-TAP) with the technical advice of the Monitoring Agricultural Resources (MARS) unit of the Joint Research Centre of the European Commission (JRC) and University of Twente.

1.1 Meteorological indices and data

Drought risk calculation at global scale is currently limited by the scarcity of reliable rainfall data (continuous time series and without large spatial gaps). For instance, the density and coverage of existing African climate data observations network have generally been described in many literatures as poor and sparse (Parker *et al.*, 2011, Washington *et al.*, 2006). One alternative to replace rainfall measurements is precipitation data generated by atmospheric circulation models and/or satellite. Examples of those data are the rainfall estimates

produced by the European Centre of Medium-Range Weather Forecast (ECMWF), the Climate Prediction Centre (CPC) of the National Oceanic and Atmospheric Administration (NOAA), the Tropical Rainfall Measuring Mission (TRMM), the Tropical Applications of Meteorology using SATellite (TAMSAT) amongst others. However, all the mentioned rainfall estimates contain errors and show deviations in different regions of the globe (Dinku et al., 2007; Feidas, 2010; Lim & Ho, 2000; Rojas et al, 2011; Sohn et al, 2010). This restriction limits the use of most of the meteorological indices developed to monitor in near real time (NTR) meteorological drought at global scale such Palmer's Drought Index (PDI) (Palmer, 1965) or the Standardized Precipitation Index (SPI) (McKee et al, 1993). Most of those drought indices will depend on the coverage of operational weather stations, the length of the time series information - at least 40-60 years are required for parameter-estimation-stability in the central part of the distribution of SPI (Guttman, 1994) - and operational communication system to release the information on time for their analysis. Unlike PDI, SPI takes into account the stochastic nature of the drought and is therefore a good measure of short (1 month) and long-term (24 month) meteorological drought. However, SPI does not account for the effect of soil, land use characteristic, crop growth, and temperature anomalies that are critical for agricultural drought monitoring (Narasimhan & Srinivasan, 2005). Crops are sensitive to soil moisture. The soil moisture deficit in the root zone during various stages of the crop growth cycle will have a profound impact on crop yield. For example, a 10% water deficit during the tasseling, pollination stage of maize could reduce the yield by as much as 25% (Doorenbos & Kassan, 1979, Hane & Pumphrey, 1984). It is not recommended to calculate the SPI on a sub-monthly basis (WMO, 2012); however crops such maize could be affected by only few days of dry spell occurrence during the flowering stage that could produce important yield reduction. In agriculture for assessing the impact of water stress, 10-day period is the most common step of analysis bearing in mind the soil water reserve and potential evapotranspiration. The Drought Monitoring Centre proposed a blending of indices to monitor the drought events in United States, (Svoboda, 2000). Using several indices (Palmer Drought Index, Vegetation Health Index, percentage of normal precipitation, daily stream flow percentiles, etc.) and ancillary indicators (SPI, snowpack conditions, groundwater levels determined from wells, in situ soil moisture measurements, etc.) from different national institutions DMC produces a final map. This approach presents the advantage to perform a holistic analysis to address meteorological, agricultural and hydrological droughts. However, due to the scarcity of reliable data needed for calculation of most drought indices, the DMC's approach has serious limitations to be applied outside developed countries. Furthermore, we can deduce that due the different nature and temporal dimension of the different type of droughts (meteorological, agricultural and

hydrological) the bleeding of indices could have some limitations of their interpretation when referring specifically to agriculture.

In summary, considering the mentioned limitations regarding: rainfall measurements (number of station and time series length without gaps), rainfall estimates by satellites or by general circulation models and the restricted use of meteorological drought indices in agriculture; we decided to explore a drought monitoring system based on vegetation indices derived from satellites.

1.2 Vegetation indices

Field studies and airborne scanner experiments (Tucker, 1979) demonstrated that the spectral reflectance properties of vegetation canopies, and in particular combinations of the red and near infrared reflectance (so called “vegetation indices” or VI), are very useful for monitoring green vegetation. Among the different VIs based on these two spectral channels, is the NDVI (Normalized Difference Vegetation Index), proposed by Deering (1978), which is the most popular indicator for studying vegetation health and crop production (MacDonald & Hall, 1980; Sellers, 1985). NDVI is affected by some well-known limitations as for example effects of soil humidity and surface anisotropy. Composite products used in most applications tend to limit these effects but they cannot be ignored completely. On the other hand, research in vegetation monitoring has shown that NDVI is closely related to the LAI (leaf area index) and to the photosynthetic activity of green vegetation. NDVI is an indirect measure of primary productivity through its quasi-linear relation with the fAPAR (Fraction of Absorbed Photosynthetically Active Radiation) (Los, 1998; Prince, 1990). Amongst vegetation indices for ASIS we selected the Vegetation Health Index (VHI) based on NDVI time series information (Kogan, 1995). This index was successfully applied in many different environmental conditions around the globe, including Asia, Africa, Europe, North America and South America (Kogan et al., 2005; Ramesh et al., 2003, Salazar et al., 2007, Seiler et al., 2007). Vegetation indices presents the advantage when compare with rainfall measurements and estimations that they are a direct measures of the ground vegetation situation when the sky is clear, resolution (from 16k until 50 m), timely information and an indirect measure of the soil ´s properties and water availability to the plants.

The objective of this paper is to describe the FAO’s agricultural drought monitoring system based on earth observation data. The “expert-system” would mimic the analysis that a remote sensing expert normally do

and simplify the results to the end-users. ASIS will provide a map every ten-day in which the GIEWS officers detect “hot spots” for every region of the world where crops may be affected by drought during the crop season. To reduce the number of false alerts due to external factors such as atmospheric perturbations, the officers would verify the “hot spots” detected by ASIS with auxiliary information, such contacting the Ministry of Agriculture or by monitoring prices of the commodities.

2. Materials and methods

2.1. Data

The main data used for this study are existing long term time series of:

- The Normalized Difference Vegetation Index (NDVI) and Brightness Temperature (BT4) from Advanced Very High Resolution Radiometer sensor on board of the National Oceanic and Atmospheric Administration (NOAA-AVHRR); 16 km resolution weekly for the period 1985-2011.
- The Normalized Difference Vegetation Index (NDVI) and Brightness Temperature (BT4) from the Meteorological Operational satellite programme (METOP-AVHRR); 1 km resolution, dekadal, since March 2007.
- The Normalized Difference Vegetation Index (NDVI) from the Satellite Pour l'Observation de la Terre Vegetation (SPOT-VGT); 1 km resolution, dekadal, for the period 1998-2011

For combining the advantage of the high resolution of METOP-AVHRR images (1 km) and the longest series of measurements of NOAA-AVHRR (from 1984, 16 km) we simulate METOP-AVHRR images based on NOAA-AVHRR data. The long term average of METOP is calculated over the period march 2007- end 2011 and the simulation of METOP images is done for the period 1984-2011. Details of the simulation method and main algorithms used in ASIS to smooth and/or correct pixels when covered by clouds are described by Van Hoolst, et al. (2015). Two additional spatial data sources were used for aggregating the final Vegetation Health Index (VHI) over space: a global crop mask and administrative regions boundaries. The MARS Unit of JRC has produced a global crop mask at 250 m, combining existing land cover/land use maps. The main use of such mask is to allow extracting from high temporal resolution satellite images, vegetation temporal profiles and differences/anomalies indicators which will be better representative of the agricultural conditions. The methodology to produce the

crop mask is described by Vancutsen *et al* (2013) for the case of African continent. The global crop mask was slightly modified based on the field experience of regional GIEWS officers. The Department of Agriculture, Fisheries and Forestry of Australian Government, ABARES contributed with the crop mask of Australia. The administrative regions were obtained from the Global Administrative Unit Layers (GAUL) database, in this study we used the version released in 1998. GAUL is an initiative implemented by FAO funded by the European Commission. It aims at providing the most reliable spatial information on administrative units for all the countries in the world. Here we used the first and second sub-national administrative units (level 1 and 2) in order to have a homogeneous reference layer a global scale. This implies that according to the different political organizations of each country, the size of individual units is highly variable.

2.2. Methodology

2.2.1. Vegetation Health Index (VHI)

First attempt of the methodology of ASIS has been described by Rojas *et al.* (2011). This study was mainly based on the 16 km resolution weekly composite images derived from NOAA-AVHRR, provided freely by NOAA's Center for Satellite Applications and Research (STAR). The results were presented at GAUL level 1. The study was limited to the African continent and it was made as a "single shot" exercise. On the other hand in ASIS the analysis is operational a near real time (every 10-day) a global level at 1 km resolution and the results are expressed at GAUL level 2 <http://www.fao.org/giews/earthobservation/>.

In ASIS, for drought assessment we selected the Vegetation Health Index (VHI) developed by Kogan (1995, 1997). VHI is a composite index joining the Vegetation Condition Index (VCI) and the Temperature Condition Index (TCI). The VCI (Kogan, 1994) is derived from the Normalized Difference Vegetation Index (NDVI). It is a scaling of the NDVI between its maximum and minimum value, and can be expressed as:

$$VCI_i = 100 * (NDVI_i - NDVI_{min}) / (NDVI_{max} - NDVI_{min}) \quad (1)$$

where $NDVI_i$ is the smoothed 10-day NDVI, and $NDVI_{max}$ and $NDVI_{min}$ are absolute maximum and minimum NDVI, respectively, calculated for each pixel and dekad during the period 1984–2016 of the smoothed NDVI. VCI was designed to separate the weather related component of NDVI from ecological factors (Kogan, 1994).

The TCI algorithm is similar to VCI, but relates to the brightness temperature T estimated from the thermal infrared band of AVHRR (channel 4). Kogan (1995) proposed this index to remove the effects of cloud

contamination in the satellite assessment of vegetation condition due to the fact that the AVHRR channel 4 is less sensitive to water vapor in the atmosphere compared with the visible light channels. High temperatures in the middle of the season indicate unfavorable or drought conditions while low temperature indicates mostly favorable conditions (Kogan, 1995). The expression consequently is:

$$TCI_i = 100 * (T_{max} - T_i) / (T_{max} - T_{min}) \quad (2)$$

VHI is expressed as:

$$VHI_i = a * VCI_i + (1-a) * TCI_i; \quad (3)$$

It is the additive combination of VCI and TCI for dekad *i*. In some studies different weights (*a* and *1-a*) are assigned to VCI and TCI. For example, Unganai and Kogan (1998) determined the weights based on the correlation between VCI and TCI with maize yield anomalies. In near normal conditions, vegetation is more sensitive to moisture during canopy formation (leaf appearance) and to temperature during flowering. Since moisture and temperature contribution during the crop cycle is currently not known, we assume that the share of dekadal VCI and TCI is equal (*a*=0.5). VHI approach needs at least 30 years of data to guarantee that each pixel examined at global level has in his “long-term memory” registered an extreme drought event. Recent satellites such MODIS or SPOT-VGT launched in the late 90’s have the disadvantage of the short time series that would under/over-estimate drought when using VHI approach. In the Sahel where the extreme drought events hit the region in the 80’s the use of MODIS or SPOT-VGT to calculate VHI would produce an over estimation of recent droughts.

2.2.2. Phenological model

VHI as proposed by Kogan (1997) can detect drought conditions at any time of the year. For agriculture, however, we are only interested to assess the water stress during the growing period of annual crops. To determine the growing period we first derived the start of season (SOS) and end of season (EOS) from the SPOT-VGT time series (1998-2011). The method of White et al (1997) was modified applying 25% of maximum NDVI of the time series as a threshold for SOS and 75% as a threshold for EOS; thresholds that we consider more appropriate for defining the growing period of annual crops. We decide to work with fixed SOS/EOS-values per pixel calculated on the long term average (LTA) of NDVI of SPOT-VGT time series, because this probably gives more stable results instead to do as proposed by Rojas *et al.* (2011) where first derived SOS/EOS for all years, then derived the multi-annual averages. In the case of winter crops, ASIS will consider as SOS the end of the crop dormancy period. We

expect that any damage due to late hardening and frost kill temperatures will be captured by the vegetation indices after dormancy period when crops re-grow in spring.

2.2.3. Calculation of the agriculture stress index (ASI)

The first step of ASI is to calculate a temporal average of the VHI assessing the intensity and duration of dry periods occurring during the crop cycle at pixel level (temporal aggregation). The second step is the calculation of the percentage of agricultural area affected by drought at administrative unit level (pixels with $VHI < 35$ – a value identified as critical in previous studies by Kogan (1994)) to assess the extent of the drought (spatial aggregation). Finally, the whole administrative unit (GAUL 2) is classified according to the percentage of affected area. The process outlined in Fig. 1. The final temporal and spatial aggregation at administrative unit has the advantage to coincide with the same unit that agricultural statistics are collected. This issue gives the possibility to use ASI as independent variable to correlate with crop yield data. The regression model could be used for crop yield forecasting and for implementing remote sensing index based crop insurance. Furthermore the relation could be used to relate with the drought management plans to use as a trigger to implement the mitigation activities to reduce the impact of drought in agriculture.

Progress of season (POS)

To help the user with the interpretation of the ASI's results in real time (10-day) it was developed an index expressed in percentage that gives an indication of the progress of the current crop season under analysis: POS (progress of season) . Approximately interpretation of the POS for a hypothetical crop is: 0% season not yet started; 1-20% emergence stage; 20-50% vegetative grow stage, 51-80% flowering and grain filling and 81-100% ripening stage. Both maps (ASI and POS) will assist the user to interpret the results around the globe where different planting date and ripening stage occurred at different time during the year.

2.2.4. Learning from the past drought events

We selected some well documented droughts occurred in the past to validate the results obtained by ASIS (Table 1). An annual summary of ASI value for each crop season is calculated in June of the second year ($t+1$), when the crop cycle of the last pixel of the world is completed for the late planting in November/December of the year “t”. The final value of ASI is assigned to the year where the NDVI maximum takes place. This summary of the temporal and spatial integration is unique characteristic of ASIS that made possible to compare historical

extreme drought events using a standard methodology. In real time analysis the value of ASI is interpreted dekad by dekad which is more challenging. Nonetheless, due to the temporal and spatial integration of ASI the user would find a significant advantage in his interpretation when compare with the classical NDVI anomaly analysis without crop mask. The total area affected in the cropping areas during the first and second crop seasons are calculated at global level using as a basic unit for expressing the final results the subnational level of GAUL 2 (district level).

2.2.5. Probability mapping

In order to compute the probability of drought affecting significant portions of the agricultural area of each administrative unit, we introduced an arbitrary threshold of 10% of area affected by drought in agriculture at administrative GAUL level 2 (district-level). In practice, when over 10% of the total agricultural area of an administrative unit is affected by drought, we assume that a large number of agriculture households experience its consequences. At district level (GAUL 2) when more than 10% of agricultural area is affected by drought, we can assume to be confronted with an extreme event with serious impact on food security. We assume that the occurrence of a certain percentage of area affected by drought in year “t” is independent on climate in other years. If P is the probability of a drought event, the number n of years that the event happens in a period of N years follows a binomial distribution (Evans et al., 2000); P is estimated by $\hat{P}=n/N$ and a confidence interval for P is: (Stuart & Ord, 1991; von Storch & Zwiers, 1999)

$$P \in \hat{P} = \pm 2 \sqrt{\hat{P}(1 - \hat{P})/N} \quad (5)$$

The probability was calculated for the first and second crop seasons independently. Then the joint frequency of 10 percent of an area affected by drought during the first and/or second season was calculated. The results are expressed by an agriculture drought frequency index.

3. Results

3.1. Phenological model

Fig. 2a presents a theoretical example of NDVI profile at pixel level in which the SOS and EOS are shown; during this window, the temporal aggregation of ASI is taking place. Both parameters are derived for two crop seasons from the long time series of NDVI of SPOT-VGT at global level (Fig. 2b). The selection of fixed SOS and EOS

gives the possibility to the system of detecting late onset of the current crop season when comparing with long term average SOS. Late SOS in water limiting regions of the world such the Sahel has proved to be a good indicator of potential crop yield reduction. Furthermore, in near-real time analysis is not possible to identify when the vegetation is affected by drought at early stage or it is a late onset of the current crop season. Late onset of the rainy season is defined only when the rains are reestablished and the end of the rainy season is shifted on time; unfortunately these cases are no possible to identify in near-real time analysis at the beginning of the crop season.

3.2. Calculation of agricultural stress index at GAUL level 1 vs. GAUL level 2

Fig. 3 shows the results of ASI based on the GAUL level 1 and GAUL level 2, it is clear that GAUL level 2 provide more details about the intensity and spatial location of the agricultural areas affected by drought. In June 2013, for instance the hot spots of drought are concentrated in the southeastern part of the North Dakota in United States (Fig. 3b); when the GAUL level 1 it is used to do the spatial aggregation (Fig. 3a) those hot spots are masked given a relative “better” classification of the percentage of agricultural area affected by drought; however masking the water stress problem that appear evident a GAUL level 2. The operational ASIS is working at GAUL level 2 at FAO; levels 0 and 1 are shown in the early warning maps only as a reference to assist the user.

3.3. Real-time interpretation of ASI and the progress of season (POS)

For detecting agricultural drought hot-spots worldwide, every 10-day a new output of ASIS is automatically produced <http://www.fao.org/gIEWS/earthobservation/> Fig. 4 shows an example of the situation in the agricultural areas at the 3rd dekad of December 2015. It is well detected the areas severely affected by drought in North-eastern Brazil, Southern Africa (Angola, Namibia, Zimbabwe, Botswana, South Africa, Lesotho, Swaziland, Malawi and Mozambique) and Morocco. ASIS as a defined shows a good capability for detecting extreme agriculture drought events at global scale; GIEWS officers should complement this information with ground data to confirm the drought hot spots detected by the system.

3.4. Learning from the drought past events

Table 2 presents the selected cases of extreme drought around the globe that have been successful detected by ASIS. Fig. 5 shows a comparison between annual summary ASI of United States with maize yield as a

percentage of the 1985-90 average yield calculated by USDA (Kogan, 1995). There is a high correlation between the extreme drought hot spots detected (ASI values > 75% of area affected by drought) and the below 80% of average maize yield (1985-90). The only year in which this relationship is not evident is 1987. Fig. 6 shows the comparison between the NDVI anomaly and ASI values for the first crop season in Somalia in 2009. In NDVI anomaly analysis the user has to put consecutive images to assess the impact of below normal activity (long term average is the reference) in ASI the latter image gives the full picture of the current situation (long term minimum and maximum of last 30 years are the reference). ASI is integrated temporal and spatial using a general crop mask; facts that give an enormous advantage to the user to easily identify agricultural drought hot spots. The annual summaries of ASIS are very useful when the user is comparing historical extreme events and their impacts in agriculture; with ASIS it is possible to identify the areas affected, the extension of affectation and the intensity of each extreme event that has happened in the past.

3.5. Empirical probabilities at sub-national level (GAUL 2)

Fig. 7 shows the probabilities of exceeding the threshold of 10% of the total agricultural area affected by drought at district level (GAUL 2). The higher probabilities of droughts are localized in the western part of the United States, northern Mexico, northern Colombia, northern Venezuela, the Horn of Africa (mainly in Somalia and the Amhara region in Ethiopia), Pakistan, India, northeast China, southern Myanmar, New South Wales in Australia and in the northern border of Kazakhstan and Russia.

4. Conclusion and perspectives

In general, the developed methodology proved useful to identify on near-real time the main hot spots around the globe. The ASI and POS indices assist the food security analyst to determine the best time to launch the alert minimizing false warnings. ASI values > 50% and POS < 30% could be interpreted as a late onset of the current crop season with a likelihood of ASI to rise in the coming decades however POS > 30% should be considered as a high probable drought beginning with a very low possibility of ASI's increase when POS reach the value of 70-80%. The database of historical ASI values starting in 1984 give the possibility to identify the administrative units (GAUL 2) exposed to high risk of agricultural drought worldwide. These results should be analyzed considering socioeconomic factors, such as population increase and livelihood strategies, to have a more comprehensive

assessment of the vulnerability of local populations to these droughts. The near-real time results provide a powerful tool for early warning and agricultural drought monitoring system to ease identify drought-sensitive areas at global level. The early warning provided by ASIS each year could enables governments throughout the region to discuss and implement agricultural drought related contingency plans. The expert system running in automatic mode warrants timely analysis of the geospatial information given the possibility to the food security analyst to dedicate more time on the socioeconomic impact and implications of the drought in agriculture. Furthermore, GIEWS Earth Observation Website includes classical remote sensing products such rainfall estimates, NDVI, VCI and VHI anomalies and profiles at GAUL 1 level for each country of the world. The global ASIS will have the first update in 2018 where the JRC ´s crop mask will be replaced by the Global Land Cover-SHARE of year 2014 - Beta-Release 1.0 http://www.glcn.org/databases/lc_glcshare_en.jsp The expert system will monitor the grassland areas of the world in near-real time and it will have capabilities of forecasting at pixel level based on the historical and current information.

Based on the encourage results with global ASIS, FAO decided to develop a standalone version of ASIS to support members countries on agricultural drought monitoring activities. Country-level ASIS will be better adapted to a country ´s agricultural situation. The new tool will differs from the current global ASIS in the following ways:

- The Country-level ASIS will use crop coefficients (kc) to better model water sensitivity for each phenological stage of cultivation; in other words, it will recognize the differing sensitivity of the various phenological stages, and attaches greater importance to the flowering and grain filling phases.
- The VHI<35 threshold used in the global ASIS (identified as representing extreme drought, whereby most of the crops are expected to be totally lost) is adjusted and modified in the country-level version, with thresholds being identified for each crop based on production statistics. The country-level ASIS may also include different user-defined thresholds, depending on the user´s interest in defining extreme, severe, moderate and light drought events.
- Crop-specific land use maps available in each country replace the agricultural crop mask, which in the global version encompasses ten cereal crops. This flexibility enables greater correlation between the vegetation indices and the final crop yield.

- The country-level version will allow the user to define the basic unit of analysis (administrative or agro-ecological).
- The tool will enable the user to calculate, midway through the crop cycle, the probability that a specific pixel will be classified as drought-affected at the end of the cycle. The probability at the start of the cycle is based on the pixel's historical probability of being drought-affected, obtained from the 30-year historical series. As the agricultural season proceeds, every ten-day new information on the evolution of the vegetation at pixel level becomes available, making it possible to adjust the historical probability based on recent data. Once at least half of the crop cycle has elapsed, the omission error is reduced and the probability of correctly classifying the pixel as drought-affected or not increases. This probability of drought events will be based on the approach of Meroni et al (2014)
- Lastly, the values of the Agricultural Stress Index (ASI) would be used as independent variables to predict agricultural crop yields by multiple regression analysis. The resulting equation is incorporated into the tool and a map of the estimated yields is automatically generated. This tool will be more appropriated for the implementation of remote sensing index based crop insurance and drought management plans.

List of Figures and Tables

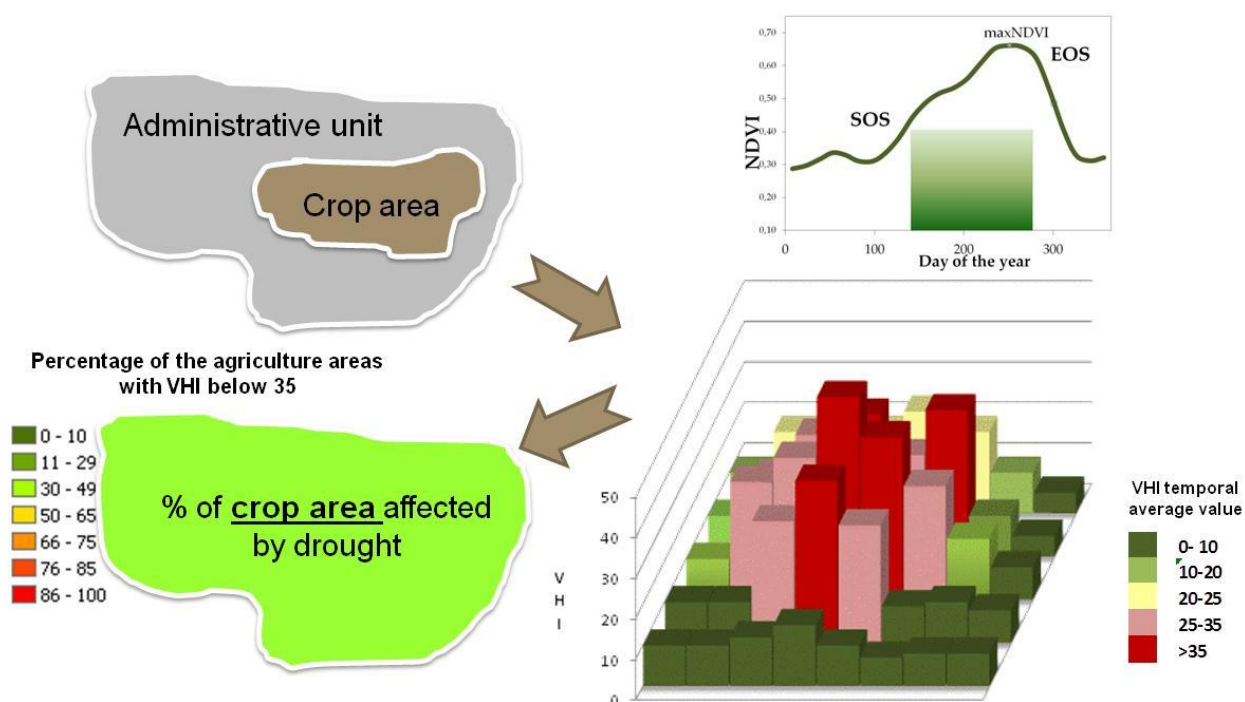


Fig. 1. The first step of ASIS is to calculate a temporal average of the VHI assessing the intensity and duration of the dry periods occurring during the crop cycle at pixel level. The second step calculates the percentage of agricultural area affected by drought at administrative unit level (pixels with $VHI < 35$), in this way assessing the extent of the drought. Finally, the whole administrative area (GAUL 2) is classified according to the percentage of area affected.

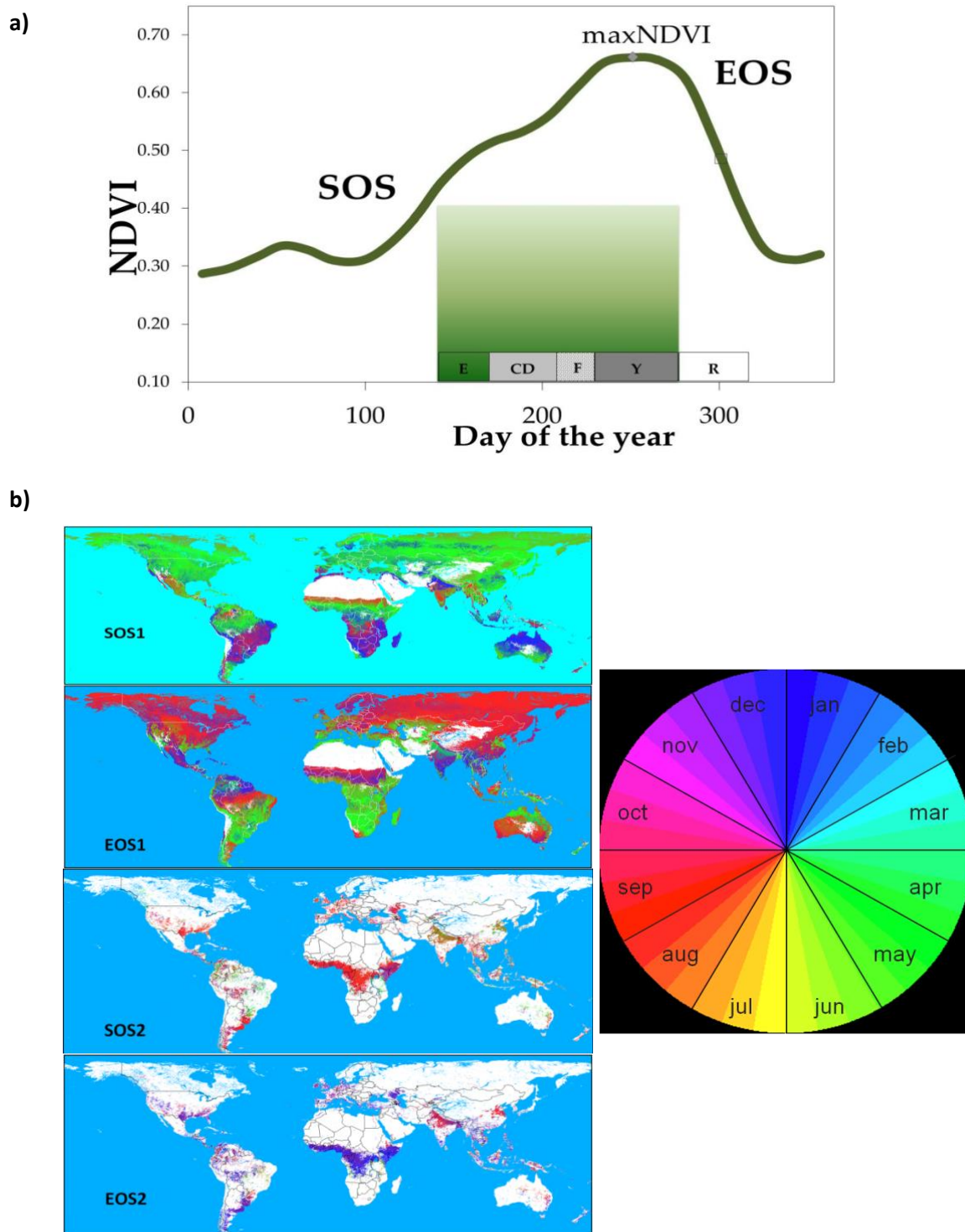


Fig. 2. a) Theoretical NDVI profile showing the period of analysis defined by the start of the season (SOS) and the end of the season (EOS). The crop cycle is divided into 5 development stages: E: establishment, CD: crop development, F: flowering, Y: yield formation or grain filling and R: ripening stage. Where CD, F and Y are the most sensitive developments to water deficit. b) Start of the season (SOS1) and end of the season (EOS1) for the first crop season and Start of the season (SOS2) and end of the season (EOS2) for the second crop season a global level based on SPOT-VGT data.

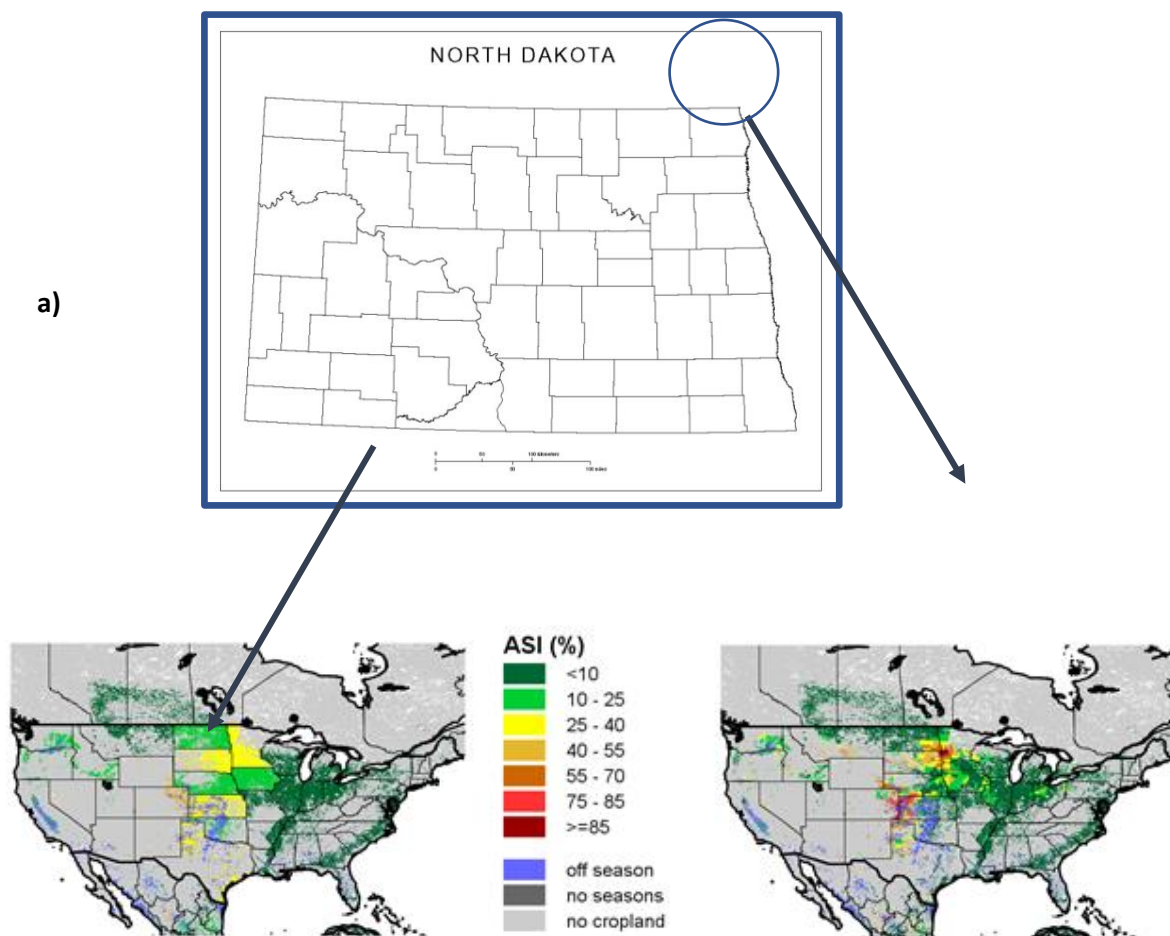


Fig. 3. Percentage of crop area (ASI) affected by drought (VHI<35) during the first crop season at the end of the third decade of June 2013 in United States. a) Results expressed using administrative level 1 of GUAL, North Dakota on the left has one category of 10-25% of agricultural area affected by drought b) Results expressed using administrative level 2 of GAUL, North Dakota on the right each county is classified on the different ASI categories of percentage of agricultural area affected by drought.

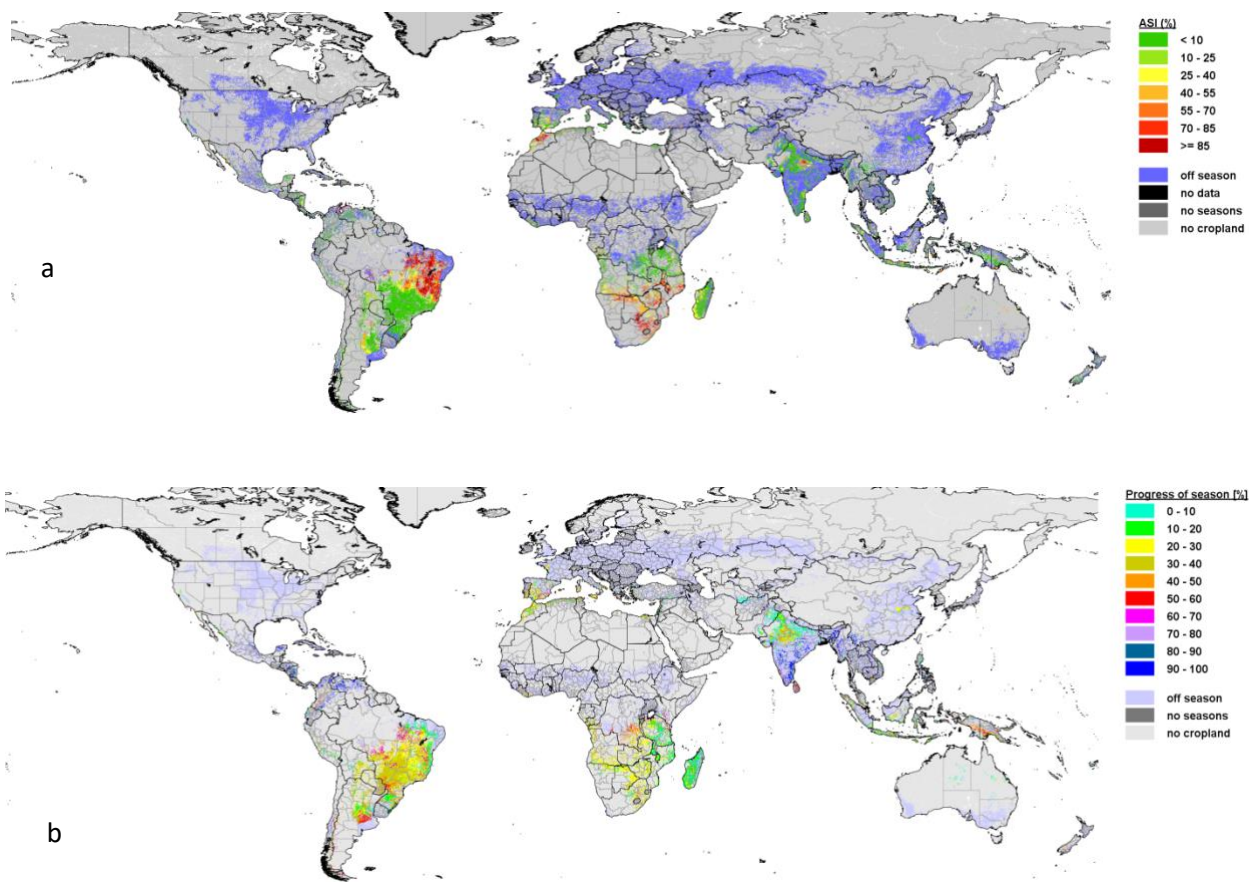


Fig. 4. a) Agricultural Stress Index (ASI) during the first crop season at the 3rd dekad of December 2015. There are three clear hot spots of drought on the agricultural areas: North-eastern Brazil, Southern Africa (Angola, Namibia, Zimbabwe, Botswana, South Africa, Lesotho, Swaziland, Malawi and Mozambique) and Morocco. b) Progress of season (POS) indicates for instance that in most of the areas affected by drought the annual crops reaching 20-30% of the crop cycle length.

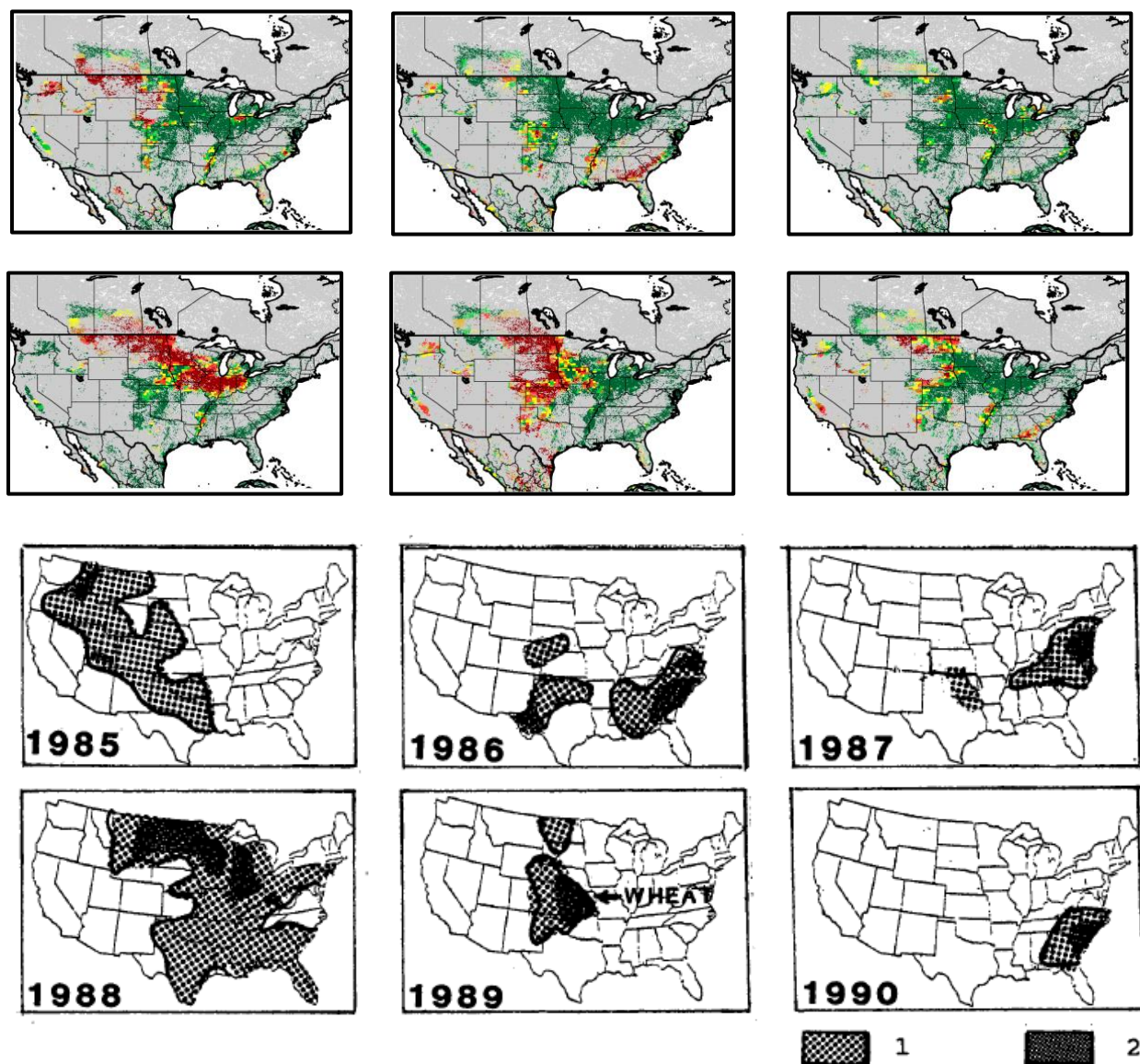


Fig. 5. a) Agricultural area affected by drought (ASI) for the first crop season of United States in 1985 to 1990 b) Maize yield as a percentage of the 1985-90 average yield calculated by USDA; first time published by Kogan (1995): 1) 80-90% 2) below 80%. For the states North Dakota, Montana, Wyoming, Oregon and Nevada wheat data were used; for Arkansas sorghum data were used.

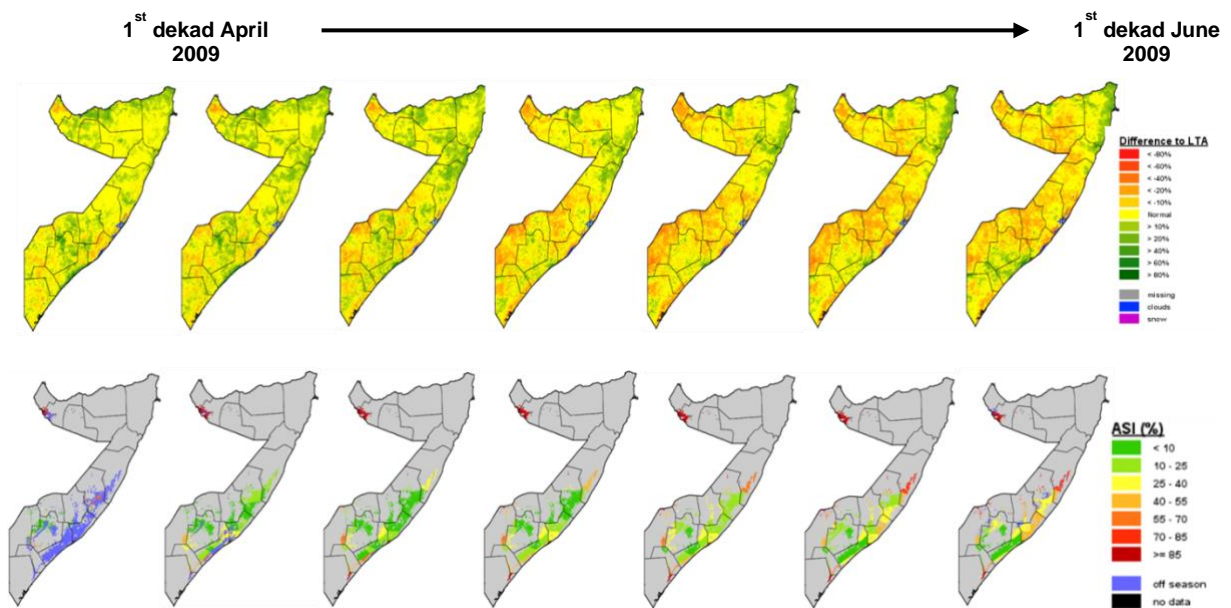


Fig. 6. Comparison between Normalized Difference Vegetation Index (NDVI) anomaly and the Agricultural area affected by drought (ASI) by dekad. The characteristics of temporal and spatial integration plus the incorporation of a crop mask on ASI facilitates the quick interpretation by the final user. Each ASI map is possible to be interpreted independently; in the case of NDVI anomaly, the user need to have the previous dekads to ensures the right interpretation of the anomaly and possible impact in agriculture.

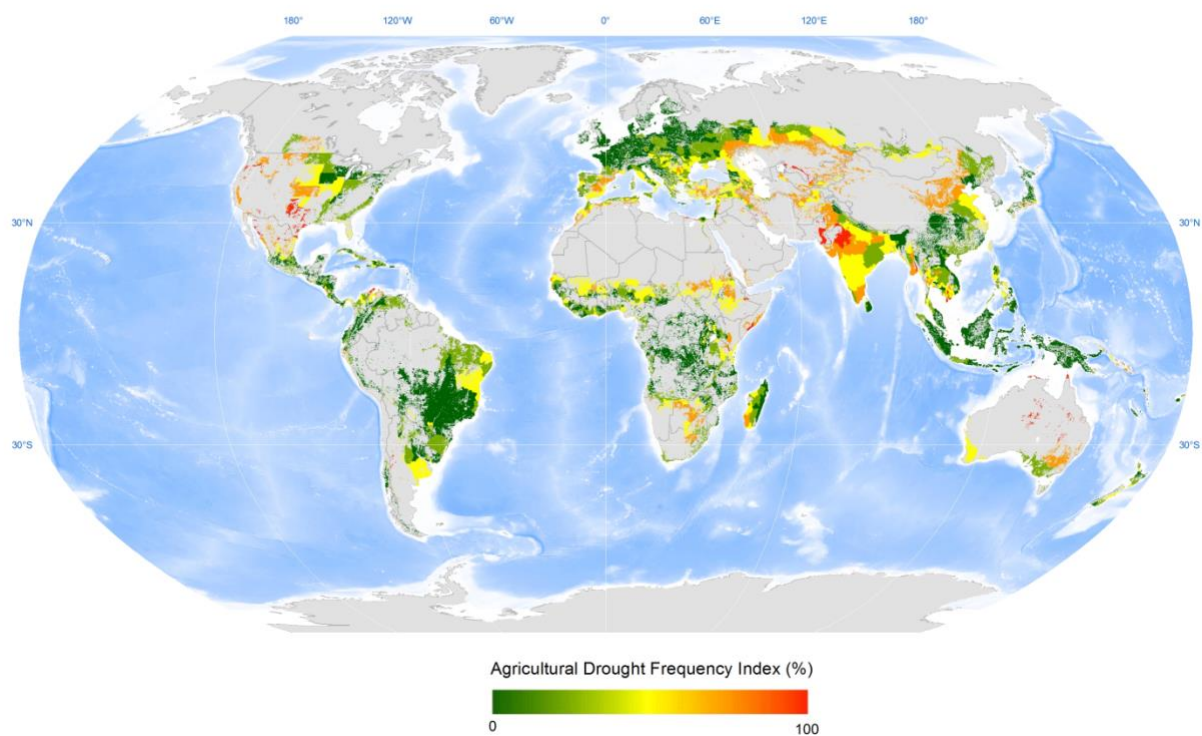


Fig. 7. Agricultural drought frequency Index of having more than 10% of agricultural area affected by drought by administrative unit (GAUL 2) during the first and second crop seasons.

Table 1. Major droughts occurred in the world during the period 1984-2014

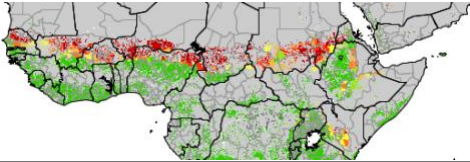
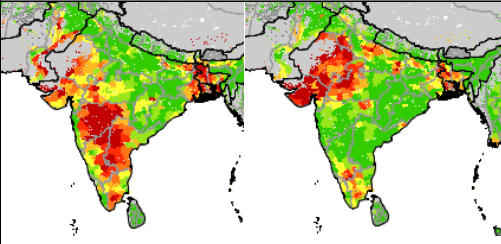
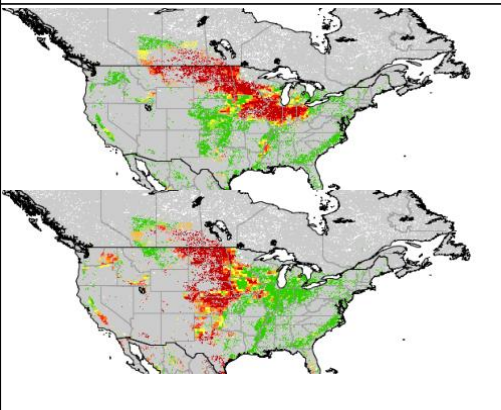
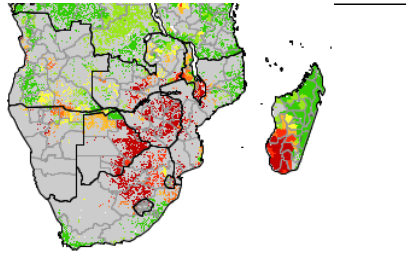
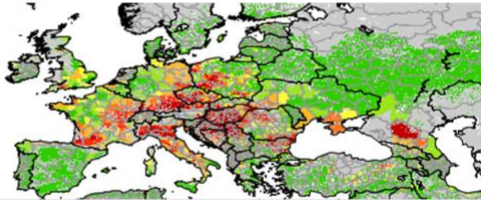
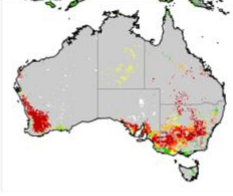
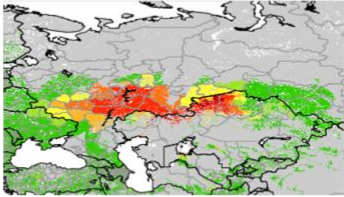
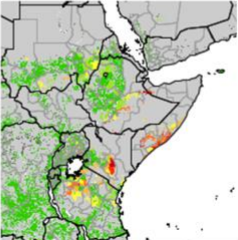
Year(s)	Country/region	Impact	ASI Map
1984	Sahel	During the crisis, an astounding 20 nations of Africa were under severe drought. Entire rivers and lakes completely dried up. Up to 20,000 people starved to death each month. Although the total number of people who perished is not completely known, it is estimated that over 1 million people died as a direct result of the drought. The worst drought in the Sahel during the early-mid 1980's occurred the year 1984 affecting most Sahel countries (Nicholson, 1985)	
1986 1987	India	In 1986 and 1987, India experienced severe drought (Nathan, 1994). During September and October 1986, the entire state of Haryana was hit by a drought. Crops like bajra, sugarcane, paddy, and pulses, worth a total of Rs. 100 crores, were damaged. In 1987, the drought situation was at its worst from June to August. Paddy sowing was done in only 40% of the area of Haryana. The 1987 drought affected 6,351 villages with a total population of more than 9 million, more than 1.4 million ha cropped area, and more than 5 million cattle. For drinking water alone, Rs. 3.70 crores assistance was given by the Indian government (Misra, 2003).	
1988 1989	United States	In the United States a severe droughts occurred during 1988 and 1989 (U.S. General Accounting Office, 1989). Following a milder drought in the Southeastern United States and California the year before, the 1988 drought spread from the Mid-Atlantic, Southeast, Midwest, Northern Great Plains and Western United States (U.S. Congress, 1988). This drought was widespread, unusually intense and accompanied by heat waves which killed around 4800 to 17000 people across the United States and also killed livestock across the United States. One particular reason that the Drought of 1988 became very damaging was farmers might have farmed on land which was marginally arable. Another reason was pumping groundwater near the depletion mark. The Drought of 1988 destroyed crops almost nationwide, residents' lawns went brown and water restrictions were declared many cities. This drought was very catastrophic for multiple reasons; it continued across the Upper Midwest States and North Plains States during 1989, not officially ending until 1990. The both droughts also affected Canada in certain divisions.	
1992	Southern Africa	The 1992 Southern African drought was the region's worst drought in living memory. Many wells and some perennial rivers dried. Well over a million cattle died: 1.03 million in Zimbabwe alone, more than 23% of the national herd (Tobaiwa, 1993). The drought affected around 86 million people in the 10 countries which then comprised SADC, of whom around 20 million people were estimated to be at 'serious risk' (SADC, 1993). Aggregate cereal production in the nine severely affected countries (including South Africa) was 38% of the previous five-year mean, and only 22% in Zimbabwe, often an exporting country. Cereal imports into the 10 SADC countries and South Africa more than tripled during 1992/3, from 3.3 to 10.5 million tonnes (Clay, 1995).	

Table 1 (continuation). Major droughts occurred in the world during the period 1984-2014

Year(s)	Country/region	Impact	ASI Map
2003	Europe	Europe experienced a particularly extreme climate event during the summer of 2003, with temperatures up to 6°C above long-term means, and precipitation deficits up to 300 mm (Trenberth et al., 2007). A record drop in crop yield of 36% occurred in Italy for maize grown in the Po valley, where extremely high temperatures prevailed (Gais et al., 2005). In France, compared to 2002, the maize grain crop was reduced by 30% and fruit harvests declined by 25%. Winter crops (wheat) had nearly achieved maturity by the time of the heatwave and therefore suffered less yield reduction (21% decline in France) than summer crops (e.g., maize, fruit trees and vines) undergoing maximum foliar development (Gais et al., 2005). Forage production was reduced on average by 30% in France and hay and silage stocks for winter were partly used during the summer (COPA COGECA, 2003b). Wine production in Europe was the lowest in 10 years (COPA COGECA, 2003a). The (uninsured) economic losses for the agriculture sector in the European Union were estimated at €13 billion, with largest losses in France (€4 billion) (Sénat, 2004).	
2006	Australia	2006 was an exceptionally dry year in many parts of the south-eastern quarter of Australia, extending north to southern Queensland, as well as in the south-east of Western Australia. The affected areas included the bulk of Australia's population, and most of its cropping areas. The annual rainfall in 2006 was 40-60% below normal over most of the country south of the Tropic of Capricorn and eastwards from central South Australia (Australian Bureau of Statistics, 2008) http://www.abs.gov.au/ausstats/abs@.nsf/0/CCC8EAD2792BC3C7CA2573D200106BDE?opendocument	
2010	Russia	Russia's worst drought in at least 50 years, drove wheat prices to the biggest jump since 1973. This is the first time in 50 years that the Hydrometeorological Center of Russia register the combination of such a long period of abnormal heat and both atmospheric and soil drought. Russia's Grain Union has said the drought is the worst since record-keeping started 130 years ago. http://www.bloomberg.com/news/articles/2010-08-03/worst-russian-drought-in-50-years-threatens-more-crops-grain-sowing-plans#news/articles/2010-08-03/worst-russian-drought-in-50-years-threatens-more-crops-grain-sowing-plans	
2011	Horn of Africa	Between July 2011 and mid-2012, a severe drought affected the entire East Africa region (OCHA, 2011). Said to be "the worst in 60 years", the drought caused a severe food crisis across Somalia, Djibouti, Ethiopia and Kenya that threatened the livelihood of 9.5 million people (Wooldridge, 2011). Many refugees from southern Somalia fled to neighboring Kenya and Ethiopia, where crowded, unsanitary conditions together with severe malnutrition led to a large number of deaths. Other countries in East Africa, including Sudan, South Sudan and parts of Uganda, were also affected by a food crisis (Wooldridge, 2011; Gordts, 2011; FEWSNET, 2011).	

References

Australian Bureau of Statistics (2008). Year Book Australia.

<http://www.abs.gov.au/ausstats/abs@.nsf/0/CCC8EAD2792BC3C7CA2573D200106BDE?opendocument>

Brown, B. (8 July 2011). "Horn of Africa drought: 'A vision of hell'". BBC News. Archived from the original on 10 July 2011. Retrieved 12 July 2011.

Ciais, Ph., Reichstein, M. Viovy N., Granier A., Ogee J., Allard V., Aubinet M. (2005). Europe-wide reduction in primary productivity caused by the heat and drought in 2003. *Nature* 437, 529-533 (22 September 2005) | doi:10.1038/nature03972.

Clay, E. (1995) 'Evaluation of ODA's response to the 1991-92 Southern Africa drought, ODA.

COPA COGECA, 2003a: Assessment of the impact of the heat wave and drought of the summer 2003 on agriculture and forestry. Committee of Agricultural Organisations in the European Union General Committee for Agricultural Cooperation in the European Union, Brussels, 15 pp.

COPA COGECA, 2003b: Committee of Agricultural Organisations in the European Union General Committee for Agricultural Cooperation in the European Union, CDP 03 61 1, Press release, Brussels.

Deering, D. W. (1978). Rangeland reflectance characteristics measured by aircraft and spacecraft sensors. Ph.D. Dissertation, Texas A&M University, College Station, TX, 388 pp.

Dinku, T., Ceccato, P., Grover-Kopec, E., Lemma, M., Connor, S. J., & Ropelewski, C. F. (2007). Validation of satellite rainfall products over East Africa's complex topography. *International Journal of Remote Sensing*, 28(7), 1503–1526.

Doorenbos, J., & Kassam, A. (1979). Yield response to water. FAO Irrigation and Drainage Paper No. 33. Rome: FAO 200 pp.

Evans, M., Hastings, N., & Peacock, B. (2000). Statistical distributions, 3rd ed. New York: John Wiley and Sons (Chapter 6).

Feidas, H. (2010). Validation of satellite rainfall products over Greece. *Theoretical and Applied Climatology* (2010) 99:193–216. DOI 10.1007/s00704-009-0135-8

FEWS-Net (24 June 2011). "East Africa: Famine warning for southern Somalia". FEWS-Net. Retrieved 14 July 2011.

Gordts, Eline (16 July 2011). "Somalia Food Crisis One Of Biggest In Decades: U.S. State Department Official". Huffington Post (USA). Retrieved 16 July 2011.

Guttman, N.B. (1994). On the sensitivity of sample L moments to sample size. *Journal of Climatology*, v34, p. 113-121.

IPCC. (2012). *Managing the Risks of Extreme Events and Disasters to Advance Climate Change Adaptation*. A Special Report of Working Groups I and II of the Intergovernmental Panel on Climate Change. Cambridge University Press, Cambridge, UK, and New York, NY, USA, 582 pp.

Kogan, F. (1994). Droughts of the late 1980's in the United States as derived from NOAA polar-orbiting satellite data. *Bulletin of the American Meteorological Society*, 76(5), 655–668.

Kogan, F. (1995). Application of vegetation index and brightness temperature for drought detection. *Advances in Space Research*, 15, 91–100.

Kogan, F. (1997). Global drought watch from space. *Bulletin of the American Meteorological Society*, 7(4), 621–636.

- Kogan, F., Yang, B., Guo, W., Pei, Z., & Jiao, X. (2005). Modelling corn production in China using AVHRR-based vegetation health indices. *International Journal of Remote Sensing*, 26(11), 2325–2336.
- Lim, H. S., & Ho, C. H. (2000). Comparison of tropical rainfall between the observed GPCP data and the assimilation products of ECMWF, NCEP/NCAR, and NASA-GEOS- 1. *Journal of the Meteorological Society of Japan*, 78(5), 661–672.
- Los, S. O. (1998). Linkages between global vegetation and climate. An analysis based on NOAA Advanced Very High Resolution Radiometer data. Ph.D. dissertation, Vrije Universiteit, Goddard Space Flight Centre, Greenbelt Maryland.
- MacDonald, R. B., & Hall, F. G. (1980). Global crop forecasting. *Science*, 208(4445), 670–679.
- McKee, T., Doesken, N., Kleist, J. (1993). The relationship of drought frequency and duration to time scales. Preprints, Eighth Conf. on Applied Climatology, Anaheim, CA, Amer. Meteor. Soc. 179-184.
- Meroni, M., Fasbender, D., Kayitakire, F., Pini, G., Rembold, F., Urbano, F., & Verstraete, M. (2014). Early Detection of Biomass Production Deficit Hot-Spots in Semi-Arid Environmental Using FAPAR Time Series and a Probabilistic Approach. *Remote Sensing of Environment* 142:57-68 doi: 10.1016-j.rse.2013.11.012.
- Misra, R.P. (2003). Managing droughts in India: Experiences and Prospects. In: *Public Governance and Decentralisation; Essays in honour T.N. Chaturvedi*. Bali, Nagar, New Delhi. 1,153 p.
- Narasimhan, B. & Srinivasan, R. (2005). Development and evaluation of Soil Moisture Deficit Index (SMDI) and Evapotranspiration Deficit Index (ETDI) for agricultural drought monitoring. *Agricultural and Forest Meteorology*, Volume 133, Issues 1–4, 69–88.

- Nathan, K. (1994). Poor Water Resources and Drought in the Gujarat/Saurashtra Regions of India. Drought Network News (1994-2001). National Drought Mitigation Center, University of Nebraska. Paper 58. <http://digitalcommons.unl.edu/droughtnetnews/58>
- Nicholson, S. 1985. Sub Saharan Rainfall 1981-1984. *Journal of Climate and Applied Meteorology*. Vol. 24, 1388-1391.
- OCHA (UN Office for the Coordination of Humanitarian Affairs) (10 June 2011). "Eastern Africa Drought Humanitarian Report No. 3". reliefweb.int. Archived from the original on 3 July 2011. Retrieved 12 July 2011.
- Parker, D., Good, E., and Chadwick, R. (2011). Reviews of Observational Data Available over Africa for Monitoring, Attribution and Forecast Evaluation, February 2011 - revised June 2011, Hadley Centre Technical Note 86.
- Palmer, W.C. (1965). Meteorological drought. U.S. Weather Bureau Research Paper 455, 58 pp.
- Prince, S. D. (1990). High temporal frequency remote sensing of primary production using NOAA AVHRR. *Applications of remote sensing in agriculture*, 4, 169–183.
- Ramesh, P. S., Sudipa, R., & Kogan, F. (2003). Vegetation and temperature condition indices from NOAA AVHRR data for drought monitoring over India. *International Journal of Remote Sensing*, 24(22), 4393–4402.
- Rojas, O., Rembold, F., Delincé J.& Léo, O. (2011). Using the NDVI as auxiliary data for rapid quality assessment of rainfall estimates in Africa, *International Journal of Remote Sensing*, 32:12, 3249-3265
- Rojas O., Vrieling A., & Rembold F. (2011). Assessing drought probability for agricultural areas in Africa with coarse resolution remote sensing imagery. *Remote Sensing of Environment*, 115, 343-352.
doi:10.1016/j.rse.2010.09.006

- SADC (1993), 'Assessment of the Responses to the 1991/92 Drought in the SADC region,' Food Security Technical and Administrative Unit, SADC.
- Salazar, L., Kogan, F., & Roytman, L. (2007). Use of remote sensing data for estimation of winter wheat yield in the United States. *International Journal of Remote Sensing*, 28(17), 3795–3811.
- Sellers, P. J. (1985). Canopy reflectance, photosynthesis and transpiration. *International Journal of Remote Sensing*, 6(8), 1335–1372.
- Sénat, 2004: France and the French face the canicule: the lessons of a crisis. Appendix to the Minutes of the Session of February 3, 2004. Information Report No. 195, 59-62. <http://www.senat.fr/rap/r03-195/r03-195.html>.
- Seiler, R. A., Kogan, F., Guo, W., & Vinocur, M. (2007). Seasonal and interannual responses of the vegetation and production of crops in Cordoba, Argentina assessed by AVHRR-derived vegetation indices. *Advances in Space Research*, 39(1), 88–94.
- Sohn, B. J., Hyo-Jin Han & Eun-Kyoung Seo, (2010). Validation of Satellite-Based High-Resolution Rainfall Products over the Korean Peninsula Using Data from a Dense Rain Gauge Network. *J. Appl. Meteor. Climatol.*, 49, 701–714. doi: <http://dx.doi.org/10.1175/2009JAMC2266.1>
- Svoboda, M. (2000). An introduction to the Drought Monitor. *Drought Network News*, 12, 15-20.
- Starita, J., Dahab, M. & Lenton, R. (2012). Drought hits the heartland of USA. *Stockholm Water Front*. 4 (December) 2012. 6-8 pp.
- Stuart, A., & Ord, K. (1991). *Kendall's advanced theory of statistics*. London: Griffin (Chapter 20).

Tobaiwa, C. (1993). Zimbabwe Country Assessment paper, SADC Drought management workshop, SADC.

Trenberth, K.E., P.D. Jones, P.G. Ambenje, R. Bojariu, D.R. Easterling, A.M.G. Klein Tank, D.E. Parker, J.A. Renwick and Co-authors, 2007: Observations: surface and atmospheric climate change. Climate Change 2007: The Physical Science Basis. Contribution of Working Group I to the Fourth Assessment Report of the Intergovernmental Panel on Climate Change, S. Solomon, D. Qin, M. Manning, Z. Chen, M. Marquis, K.B. Averyt, M. Tignor and H.L. Miller, Eds., Cambridge University Press, Cambridge, 235-336.

Tucker, C. J. (1979). Red and photographic infrared linear combinations for monitoring vegetation. Remote Sensing of Environment, 8, 127–150.

United States. General Accounting Office (1989). Crop Production : Outlook for Post-Drought Recovery During 1989 : Briefing Report to the Chairman, Subcommittee on Agricultural Research and General Legislation, Committee on Agriculture, Nutrition, and Forestry, U.S. Senate , June 1989, <https://fraser.stlouisfed.org/title/?id=835> , accessed on March 9, 2015.

United States. Congress. House. Committee on Banking, Finance, and Urban Affairs. Subcommittee on Economic Stabilization (1988). Impact of the Drought on Prices and Production, July 6, 1988. <https://fraser.stlouisfed.org/title/?id=836> , accessed on March 9, 2015.

Vancutsem, C., Marinho, E., Kayitakire, F., See, L., & Fritz S. (2013). Harmonizing and Combining Existing Land Cover/Land Use Datasets for Cropland Area Monitoring at the African Continental Scale. Remote Sensing 2013, 5, 19-41; doi:10.3390/rs5010019

Van Hoolst, R., Eerens, H., Haesen, D., Royer, A., Bydekerke, L., Rojas, O., Li, Y., & Racionzer, P. (2016). FAO ´s AVHRR –based Agricultural Stress Index System (ASIS) for global drought monitoring. International Journal of Remote Sensing, 37:2, 418-439, Doi: 10.1080/014331161.2015.1126378

Von Storch, H., & Zwiers, F. W. (1999). *Statistical analysis in climate research*. Cambridge: University Press (ISBN 0 521 45071 3), 484 pp.

Washington, R., Harrison, M., Conway, D., Black, E., Challinor, A., Grimes, D., Jones R., Morse A., Kay G., and Todd M. (2006). Africa climate change: Taking the short route. *Bulletin of American Meteorological Society*, 87, 1355-1366.

White, M. A., Thornton, P. E., & Running, S. W. (1997). A continental phenology model for monitoring vegetation responses to inter-annual climatic variability. *Global Biogeochemical Cycles*, 11(2), 217–234.

World Meteorological Organization (2012). *Standardized Precipitation Index. User Guide*. WMO No.1090, 16 p.

Wooldrige, M. (2011). "Horn of Africa tested by severe drought". *BBC News*. Archived from the original on 13 July 2011. Retrieved 12 July 2011.

Acknowledgements

The ASIS set-up is part of the European Union (EU)/FAO programme on “Improved global governance for hunger reduction”. FAO developed the ASIS approach to detect agricultural areas with a high likelihood of water stress (drought). VITO implemented the ASIS methodology into an operational system at the global scale, now available at FAO. Based on earth observation data, ASIS will support the vegetation monitoring activities of the FAO-Global Information and Early Warning System (GIEWS). The intellectual property rights of FAO-ASIS belong to FAO. We would like to thank Geospatial World Forum to offer to FAO the 'Geospatial World Excellence Award – 2016' for its Agriculture Stress Index System (ASIS).